Yao *et al.*
European Journal of Medical Research (2024) 29:546
https://doi.org/10.1186/s40001-024-02129-3

European Journal of Medical Research

RESEARCH

Open Access

Acute hyperglycemia exacerbates neuroinflammation and cognitive impairment in sepsis-associated encephalopathy by mediating the ChREBP/HIF-1α pathway

Peng Yao[1,2†], Ling Wu[3†], Hao Yao[2†], Wei Shen[2*] and Ping Hu[3*]

Abstract

Objectives Delirium is a prominent symptom of sepsis-associated encephalopathy (SAE) and is highly prevalent in septic patients hospitalized in the intensive care unit, being closely connected with raised mortality rates. Acute hyperglycemia (AH) has been recognized as a separate risk factor for delirium and a worse prognosis in critically sick patients. Nevertheless, the exact contribution of AH to the advancement of SAE is still unknown.

Methods This research retrospectively evaluated the connection between blood glucose levels (BGLs) and the incidence of delirium and death rates in septic patients in the ICU of a tertiary comprehensive hospital. In addition, a septic rat model was induced through cecal ligation and puncture (CLP), after which continuous glucose infusion was promptly initiated via a central venous catheter post-surgery to evaluate the potential implications of AH on SAE. Next, septic rats were assigned to four groups based on target BGLs: high glucose group (HG, ≥ 300 mg/dL), moderate glucose group (MG, 200–300 mg/dL), normal glucose group (NG, < 200 mg/dL), and a high glucose insulin-treated group (HI, 200–300 mg/dL) receiving recombinant human insulin treatment (0.1 IU/kg/min). The sham group (SG) received an equivalent volume of saline infusion and denoted the NG group. The effects of AH on neuroinflammation and cognitive function in septic rats were evaluated using behavioral tests, histopathological examination, TUNEL staining, ELISA, and Western blot. The effects of glucose levels on microglial activation and glucose metabolism following lipopolysaccharide (LPS, 1 μg/mL) exposure were assessed using CCK8 assay, qRT-PCR, Western blot, and ELISA.

Results Our findings revealed that AH during sepsis was a separate risk factor for delirium and assisted in predicting delirium occurrence. AH raised the levels of systemic and central inflammatory cytokines in septic rats, promoting neuronal apoptosis, blood–brain barrier disruption, and cognitive impairment. In addition, both in vivo and in vitro, an elevated glucose challenge increased the ChREBP, HIF-1α, glycolytic enzymes, and inflammatory cytokines expressions in microglia after exposure to CLP or LPS.

†Peng Yao, Ling Wu and Hao Yao have authors contributed equally to this work.

*Correspondence:
Wei Shen
xgsw123@outlook.com
Ping Hu
ndyfy10095@ncu.edu.cn
Full list of author information is available at the end of the article

Conclusions These results collectively suggest that hyperglycemia can exacerbate neuroinflammation and delirium by enhancing microglial glycolysis under septic conditions, potentially mediated by upregulation of the ChREBP/HIF-1α signaling pathway.

Keywords Hyperglycemia, Sepsis-associated encephalopathy, Microglia, Metabolic reprogramming, HIF-1α, ChREBP

Graphical abstract

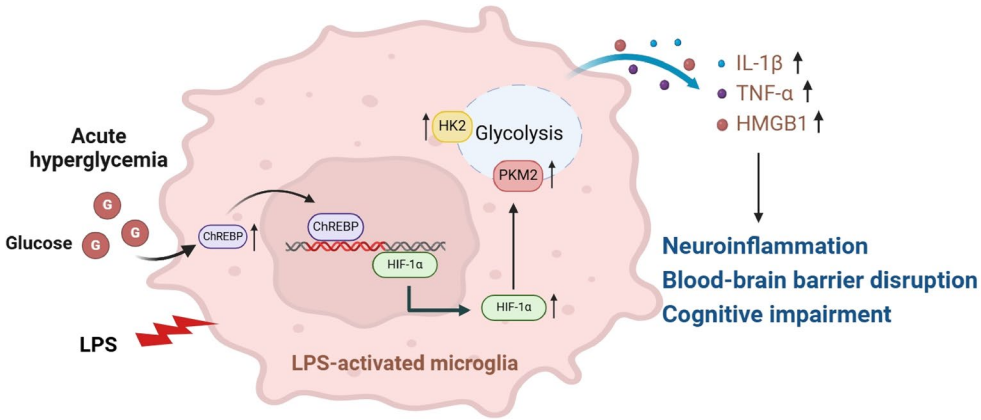

Introduction

Sepsis-associated encephalopathy (SAE) is an acute diffuse brain dysfunction syndrome that occurs as a result of sepsis [1], characterized by altered consciousness, with 30–70% of sepsis cases progressing to SAE [2]. It is closely associated with ICU-acquired weakness, deterioration of motor and sensory functions, and long-term cognitive impairments, severely impacting the independent living capability of sepsis survivors [3]. The pathophysiological alterations responsible for SAE are intricate and multifaceted, encompassing the activation of microglial cells, breakdown of the blood–brain barrier (BBB), and metabolic reprogramming [4, 5].

During sepsis, the incidence of acute hyperglycemia (AH) is approximately 40%, hypothesized to be induced by intricate interactions involving cortisol, catecholamines, and cytokines, eventually culminating in metabolism disorders and insulin resistance [6, 7]. Short- and long-term abnormalities in glucose metabolism have been reported to be closely associated with neuroinflammatory-related neurodegenerative diseases [8, 9]. The correlation between AH and adverse outcomes, such as delirium and higher mortality rates, is particularly significant in non-diabetic individuals with severe circumstances, including sepsis and traumatic brain injury [10]. Further research revealed that hyperglycemia can exacerbate the infection-induced immuno-inflammatory response and is associated with macrophage/microglial activation [11, 12]. Nevertheless, the precise processes have still to be clarified.

Microglia, the main innate immune cells in the central nervous system (CNS), possess a critical function in the neuroinflammatory response that occurs during sepsis [13]. When stimulated by LPS or pro-inflammatory cytokines, microglia undergo M1 activation and synthesize various pro-inflammatory mediators [14], encompassing IL-1β and TNF-α. In addition, glucose metabolism shifts from oxidative phosphorylation (OXPHOS) toward aerobic glycolysis [15], thereby playing a pivotal role in the early host defense against pathogenic invasion [16]. However, sustained overactivation of microglia leads to neuronal death or apoptosis [17]. However, pharmacological inhibition of glycolytic enzymes can attenuate microglial M1 polarization and neuroinflammation [18].

HIF-1α, a key transcription factor associated with the Warburg effect, is involved in regulating microglial metabolic reprogramming [19]. In addition to hypoxia, challenges such as LPS and high glucose can also stabilize and activate HIF-1α and elevate the downstream target gene expression, comprising HK2 and PKM2 [20]. Meanwhile, HIF-1α knockout suppresses the secretion of the pro-inflammatory cytokine and enhances the survival outcomes of septic mice [21]. Carbohydrate response elements (ChRE)-binding protein (ChREBP) is an essential regulatory factor involved in sensing and glucose

metabolism [22]. HIF-1α gene promoter contains multiple ChRE sequences and exhibits a strong induction response to hyperglycemia [23, 24]. Considering the overlap of target genes between HIF-1α and glucose-related metabolic disorders, HIF-1α may potentially promote the progression of SAE under hyperglycemic conditions. Although a recent study demonstrated enhanced HIF-1α expression in neurons of rats subjected to high glucose levels [25], the mechanisms and functional relevance remain unknown.

Thus, we aimed to ascertain the connection between blood glucose levels (BGL) and delirium during sepsis. In addition, the impact of AH on neuroinflammation, cellular damage, and metabolic reprogramming following the onset of sepsis was explored both in vivo and in vitro, as well as potential mechanisms.

Materials and methods

Study design and patients

In this retrospective research, adult septic patients hospitalized in the intensive care unit (ICU) between January 2022 and January 2024 were screened, as depicted in Supplementary Fig. 1. The criteria for inclusion were outlined below: (1) The clinical diagnosis of sepsis based on the Sepsis 3.0 criteria [26]; (2) age ≥ 18 years; (3) ICU stay ≥ 24 h. The criteria for exclusion were as follows: (1) acute brain injury, encompassing epilepsy, traumatic brain injury, intracranial infection, ischemic stroke, or hemorrhagic stroke; (2) psychiatric disorders or neurological diseases; (3) chronic alcoholism or substance abuse; (4) hepatic encephalopathy, hypoglycemic coma, metabolic encephalopathy, or additional severe liver or kidney dysfunction impacting consciousness; (5) severe electrolyte disturbances; (6) pulmonary encephalopathy or $PaCO_2 \geq 80$ mmHg; and (7) acute or chronic liver dysfunction, including hepatic encephalopathy and cirrhosis.

Data within the first 24 h upon admission were collected, including BGLs and information on insulin treatment. Patients experiencing severe hyperglycemia (≥ 300 mg/dL) at least twice were administered insulin at a rate of 0.1–0.5 IU/kg/min and included in the HG group; patients experiencing moderate hyperglycemia (200–300 mg/dL) at least twice were included in the MG group; and patients with BGLs below 200 mg/dL and not requiring insulin treatment were included in the NG group. During hospitalization, delirium occurrence was assessed twice daily by two senior nurses, who were blinded to the study protocol, employing the Confusion Assessment Method for the Intensive Care Unit (CAM–ICU). This work was approved by the Ethics Committee of the First Affiliated Hospital of Nanchang University.

Baseline data, encompassing age, gender, diabetes history, site of infection, renal replacement therapy, APACHE II score, SOFA score, mechanical ventilation, vasopressors, ICU stay, and occurrence of delirium, were collected for all enrolled patients.

Rats and *sepsis* models

We obtained a cohort of healthy male Sprague–Dawley (SD) rats weighing between 200 and 240 g, between 12 and 14 weeks, from Vital River Lab Rotary in Zhejiang, China. The subjects were subjected to controlled environmental settings, which included a temperature range of 23–25 °C, humidity levels maintained between 50 and 60%, a 12-h light/dark cycle, and unrestricted availability of food and water. The handling and experimentation of animals were performed in complete compliance with the rules established by the Animal Welfare Ethics Committee of Nanchang University.

Following a 1-week acclimatization period, the rats underwent right jugular vein catheterization. A PE-50 catheter, having an inner diameter of 0.58 mm and an outside diameter of 0.99 mm, was placed into the jugular vein to assist in delivering the specified solution. Subsequently, the catheter was tunneled through a posterior neck incision and connected to a swivel harness, enabling the rats to move freely within their cages while maintaining access to the administered solution.

After catheterization, the SAE model was created by performing cecal ligation and puncture (CLP), as explained in prior research. In summary, the rats were administered 50 mg/kg of pentobarbital to induce anesthesia and a 1.5 cm incision was done along the midline to subject the cecum. Next, the cecal ileocecal valve was double-ligated at the distal one-third of the cecum. Subsequently, an 18G needle was utilized to puncture the cecum, causing a small quantity of intestinal detritus to be expelled into the abdominal cavity. Following the surgical procedure, the rats were put on a heating blanket set at a temperature of 37 °C and observed until they regained consciousness from the effects of the anesthetic. The rats in the SG were subjected to cecal exposure without CLP. Following the CLP operation, blood samples were obtained every 3 h from the right jugular vein catheter for blood glucose analysis.

Animal treatment

The rats were first allocated into two primary groups: the CLP group and the SG. Preliminary experiments were conducted to establish the optimal amount of glucose required to attain certain goal BGLs in the past. The rats were allocated into three subgroups based on their target levels. The high glucose group (HG, $n = 15$) obtained a continuous intravenous infusion of 0.9% saline with 27% glucose (w/v) at a rate of roughly 39 mg/(kg·min) to preserve BGLs over 300 mg/dL. The moderate glucose group

(MG, $n=15$) acquired a continuous intravenous infusion of 0.9% saline that included 18% glucose (w/v) at a rate of about 24 mg/(kg·min) to preserve BGLs between 200 and 300 mg/dL; the none glucose group (NG, $n=15$), wherein rats received an intravenous infusion of an equivalent volume of 0.9% saline, maintaining BGLs below 200 mg/dL; and the HG group treated with recombinant human insulin (HI, $n=15$) at a dosage of 0.1 IU/kg/min to maintain BGLs between 200 and 300 mg/dL. In contrast, rats in the SG ($n=8$) received an infusion of 0.9% saline at a volume equivalent to the other groups. Following the CLP procedure, the designated solution was continuously administered through a central vein catheter for 9 h.

Y-maze

48 h after CLP, the spatial working memory of rats was evaluated utilizing the *Y*-maze (Shanghai XinRuan, China), which consisted of three black polypropylene arms labeled A, B, and C, with each arm measuring $40\times10\times16$ cm and placed at an angle of 120° from each other. During the 8-min experimental phase, the rats were given unrestricted access to explore the labyrinth. They were placed at the far end of any arm, and their entries and exits into each arm were recorded. For an entry or exit to be counted, all four limbs of the rat had to enter or exit an arm. A sequence of three different arm entries (such as ABC, CAB) was considered as spontaneous alternation performance (SAP), which reflects good working memory. The movement of a rat transitioning from one arm to the central region and then returning to the same arm was recorded as a same-arm return (SAR) each time. The alternation percentage was computed as [number of alternations/(total number of arm entries-2)] $\times$ 100. Following each experiment, the box was cleaned with 75% alcohol.

Novel object recognition (NOR) test

The NOR test was employed to assess alterations in short-term memory. In a plastic box with a side length of 40 cm, two objects of identical size and material (Object A) were placed. Prior to the test day, the rats were acclimated to the test box for 10 min. During the testing day, one of the objects, A (familiar object, *F*), was replaced with a similar-sized material object, B (novel object, *N*). Subsequently, the rats were individually introduced inside the enclosure and given unrestricted access to examine the items for 5 min. Subsequently, the box was cleaned using a solution of 75% alcohol. Object exploration was stated as orienting the nose toward an object at a distance $\leq$ 2 cm. The exploration times for the familiar and novel objects were recorded, and the discrimination index (DI) was computed as $(t[N\text{-}F])/(t[F+N])\times100\%$.

Evans blue (EB) staining

2 h prior to measurement, a 2% solution of EB was intravenously injected at a dose of 4 mL/kg. Following anesthesia with 5% pentobarbital sodium (50 mg/kg), rats underwent cardiac perfusion with saline. Tissue samples were homogenized in 5 mL of 0.1 M PBS, mixed with 5 mL of 60% trichloroacetic acid, underwent centrifugation at 4000 rpm for 15 min, and the supernatant was gathered. A spectrophotometer was employed to determine the supernatant's absorbance at 620 nm. Finally, the EB content in the brain tissue was calculated based on the unit weight.

Histological examination

Rats were euthanized using sodium pentobarbital after the behavioral tests, and blood and whole brain specimens were gathered. The brain specimens were preserved in a solution of 4% paraformaldehyde for 24 h. After that, they were embedded with paraffin and cut into coronal slices that were 5-μm thick. In order to perform a histological investigation, the slices were first treated to remove the paraffin and then dehydrated. Hematoxylin and eosin staining were then conducted to assess morphological changes in the hippocampal region.

For immunofluorescence analysis, the sections were subjected to antigen retrieval by immersion in sodium citrate buffer at 100 °C for 15 min. Afterward, the sections were blocked utilizing 0.01 mM PBS with 10% goat serum for 15 min. The sections were then incubated overnight at 4 °C with primary antibodies, including rabbit anti-IBA1 and CD68 (Abcam, USA), to target specific cellular markers. On the next day, the samples were rinsed three times with PBS, followed by incubation in the dark with fluorescently labeled secondary antibodies (FITC or CY3) at ambient temperature for 2 h. Subsequently, the samples were counterstained with DAPI for 10 min and sealing the tissue slices. The average number of IBA1 + CD68-positive cells in three non-overlapping areas was observed and calculated using a fluorescence microscope (ZEISS, Germany).

TUNEL staining

TUNEL staining was conducted utilizing the TUNEL Assay Kit (Beyotime Biotech, China) in accordance with the company's protocol. The sections were treated with 4% paraformaldehyde to fix them, made permeable with 0.1% Triton *X*-100 for 10 min, and then subjected to the TUNEL reaction mixture for 1 h at 37 °C in a lack of light. DAPI was employed to stain the cell nuclei. Imaging was performed using an optical microscope (Olympus, USA).

Cell culture and treatment

BV2 cells (obtained from the Pricella Life science & Technology, China) were cultivated in Dulbecco's Modified Eagle Medium (DMEM, Thermo Fisher Scientific, USA) enriched with 10% fetal bovine serum and 1% penicillin/streptomycin and maintained in a 37 °C humidified incubator with a constant oxygen supply (5% CO_2, 21% O_2, and 74% N_2). To simulate sepsis, BV2 cells underwent treatment with 1 μg/mL LPS and then incubation in DMEM supplemented with 5.6 mM (LG group), 16.7 mM (MG group), and 25.0 mM (HG group) glucose. BV2 cells were pretreated with 10 μM KC7F2, followed by 1 μg/mL LPS and/or 25.0 mM glucose for the cellular signaling pathway study.

shRNA-mediated ChREBP knockdown

The lentiviral vectors for the knockdown of ChREBP (sh-ChREBP) or the non-silencing control shRNA (NC) were synthesized by Santa Cruz Biotechnology (cat. no. sc-3861, USA). BV2 cells were infected with lentivirus-mediated sh-ChREBP or NC for 48 h. To serve as a negative control, non-silencing shRNA was used (NC). The sh-ChREBP or non-targeting shRNA lentiviral vectors were added to DMEM at a final multiplicity of infection of 50. Stable transformed cell lines were subsequently screened using puromycin (5 μg/mL). Silencing efficiency was assessed by Western blot.

Cell viability

BV2 cells were placed in a 96-well plate and subjected to 1 μg/mL LPS for a duration of 12 h. Subsequently, a predetermined amount of glucose was introduced into the wells. Afterward, 10 μL of CCK-8 solution was introduced according to the manufacturer's recommendations (Beyotime, China). Afterward, the plate was put in a humidified incubator that was adjusted at 37 °C for 1 h. Following incubation, the plate's absorbance was measured at 450 nm utilizing a microplate reader.

ELISA

The IL-1β, TNF-α, HMGB1, NSE, and S100β levels were ascertained by employing a commercial ELISA kit following the manufacturer's recommendations (Elabscience, China). After collecting blood samples or hippocampal tissue homogenate from animal experiments, the specimens immediately centrifugated at 3000 rpm for 15 min at 4 °C, and the supernatant was gathered. For in vitro experiments, BV2 cells were initially stimulated with LPS for 12 h and subsequently exposed to 25.0 mM glucose. After collecting the supernatant, the IL-1β, TNF-α, and HMGB1 levels were measured.

Evaluation of glycolysis and metabolic pathway shift

The glycolysis/oxidative phosphorylation assay kit (DOJINDO laboratories, Japan) was employed to assess glycolysis levels and shifts in metabolic pathways. Briefly, following the methods outlined in a previous study [27], BV2 or HMGB1–shRNA/NC cells (2.0×10^4 cells/well) were seeded in a 96-well plate and subsequently treated with 1 μg/mL LPS and DMEM containing a pre-defined level of glucose for 12 h. To evaluate shifts in the metabolic pathway shift, cells were initially stimulated with LPS and subsequently treated with or without 1.25 μM oligomycin (an inhibitor of OXPHOS) for 3 h. Following this, 100 μL of ATP working solution was introduced to each well, and absorbance was quantified at 450 nm. The shift in metabolic pathways was evaluated by measuring mitochondrial ATP and glycolytic ATP production.

To examine glycolysis levels, after LPS stimulation, 20 μL of the supernatant was incubated with 80 μL of the lactate working solution for 30 min. The mixture absorbance was subsequently ascertained at 450 nm, employing a microplate reader. The glycolysis degree was assessed by measuring the lactate production.

Western blotting

The hippocampus tissues or BV2 cells were homogenized utilizing RIPA lysis buffer, aligning with the manufacturer's recommendations. The protein concentration was quantified employing a BCA assay kit (Boster, China). Then, 20 μg of protein specimens were separated employing a 10% SDS–PAGE gel and then deposited onto a PVDF membrane (MILLIPORE, USA). The membrane was subsequently obstructed with 5% skimmed milk and underwent incubation at 4 °C overnight with primary antibodies specifically targeting ZO-1, Claudin-5, IL-1β, TNF-α, HMGB1, iNOS, ChREBP, HK2, PKM2 (Abcam, USA), and β-actin (Jinqiao Biotechnology, China). It was then incubated with HRP-conjugated secondary antibodies at ambient temperature for 2 h. Finally, protein bands were observed and quantified utilizing the ChemiDoc Imaging System (Bio-Rad Laboratories, USA) and Image Lab software.

RNA extraction and real-time PCR

The TRIzol reagent (Invitrogen, Thermo Fisher Scientific, USA) was employed to extract the total RNA, while the cDNA was generated utilizing the PrimerScript reagent Kit (Takara) following the manufacturer's recommendations. The ABI StepOne real-time PCR machine (Life Technologies, USA) and the SYBR Green PCR Master Mix (TransGen Biotech, China) were deployed to

conduct real-time PCR. The PCR products were amplified, measured, and normalized utilizing β-actin as a control. All the PCR primers are provided as follow. ChREBP: Forward: 5′-CACTCAGGGAATACACGC CTAC-3′, Reverse: 5′-GGACTTCTGGGATTCTGG TTCTA-3′. β-Actin: Forward: 5′-ACCCAGAAGACT GTGGATGG-3′, Reverse: 5′-CACATTGGGGGTAGG AACAC-3′. HIF-1α: Forward: 5′-CTGGGACTTTCT TTTACCATGC-3′, Reverse: 5′-AATGGATTCTTT GCCTCTGTGT-3′. HK2: Forward: 5′-TGATCGCCT GCTTATTCACGG-3′, Reverse: 5′-AACCGCCTAGAA ATCTCCAGA-3′. PKM2: Forward: 5′-GCCGCCTGG ACATTGACTC-3′, Reverse: 5′-CCATGAGAGAAA TTCAGCCGAG-3′.

Data analysis

The Shapiro–Wilk test was applied to estimate the normality of continuous data. The Kruskal–Wallis test was applied to compare non-normally distributed continuous variables, which were expressed as the median (interquartile range [IQR]) or count (percentage). The Pearson rank correlation test was employed to analyze the link between BGLs and delirium. The study conducted logistic regression and receiver operating characteristic (ROC) analyses to assess the predictive significance of blood glucose levels in relation to the occurrence of delirium and death within 28 days. The continuous variables in both in vitro and in vivo experiments had a normal distribution and were expressed as the mean ± Standard Deviation (SD). Statistical significance was assessed utilizing either one- or two-way analysis of variance, depending on the situation. A log-rank test was implemented to evaluate the variances in survival rates among the groups.

Results

Elevated BGLs in septic patients in the ICU are linked to an elevated risk of delirium and 28-day mortality

The demographic and clinical characteristics of patients in the three groups are listed in Table 1. This study included 124 adult septic patients (63 men and 61 women) with a mean age of 59 (37–72) years, including 52 in the NG group, 49 in the MG group, and 23 in the HG group. Among the comprised patients, 104 (83.9%) survived, and 20 (16.1%) died. The incidence of delirium was 29.03%, with an average ICU stay of 8 (3–15) days. Age, gender, history of diabetes, site of infection, renal replacement therapy, mechanical ventilation, vasopressors, and ICU stay were comparable among the groups.

Overall, the findings manifested that the MG and HG groups had a significant rise in the prevalence of delirium (30.6% vs. 11.5%, $P < 0.01$; 65.2% vs. 11.5%, $P < 0.001$) and APACHE II scores (median, 19 scores

Table 1 Demographic and clinical features

Features	Sepsis with NG	Sepsis with MG	Sepsis with HG	*P* value
N	52	49	23	
Age (years)	58 (37–66)	62 (56–69)	64 (52–72)	0.101
Sex, *n* (%)				
Male	28 (53.9)	24 (49.0)	11 (47.8)	0.142
Female	24 (46.2)	25 (51.0)	12 (52.2)	0.32
Diabetes	18 (34.6)	14 (28.6)	7 (30.4)	0.005
Delirium	6 (11.5)	15 (30.6)	15 (65.2)	< 0.001
28-day mortality	4 (7.69)	9 (18.4)	7 (30.4)	< 0.001
Site of infection, *n* (%)				
Abdomen	12 (23.1)	13 (26.5)	6 (26.1)	0.301
Respiratory tract	31 (59.6)	28 (53.85)	10 (43.5)	0.112
Urinary tract	3 (5.77)	4 (8.16)	4 (17.4)	0.221
Skin/Soft tissue	2 (3.85)	1 (2.04)	2 (8.70)	< 0.001
Others	4 (7.69)	3 (6.12)	1 (4.35)	0.07
Score (IQR)				
APACHE II	15 (10–22)	19 (15–26)	24 (18–30)	< 0.001
SOFA (day 1)	7 (3–10)	11 (5–13)	12 (6–15)	< 0.001
Renal replacement therapy, *n* (%)	6 (11.5)	5 (10.2)	3 (13.0)	0.140
Mechanical ventilation, *n* (%)	33 (63.5)	29 (59.2)	8 (34.8)	0.005
Vasopressors, n (%)	29 (55.8)	27 (55.1)	6 (26.1)	< 0.001
ICU stay (days)	6 (4–11)	9 (5–13)	10 (7–16)	< 0.001
Albumin	29.43 ± 2.93	27.75 ± 3.21	23.47 ± 3.51	0.01

[IQR, 15–26] vs. 15 scores [IQR, 10–22], $P<0.01$; 24 scores [IQR, 18–30] vs. 15 scores [IQR, 10–22], $P<0.01$) contrasted with the NG group. Kaplan–Meier analysis of septic patients with different BGLs displayed that the HG group had a significant elevation in the 28-day mortality (Fig. 1a, $P<00.001$) and was comparable to the MG group and contrasted with the NG group ($P=0.142$). In addition, Pearson correlation analysis determined that BGLs within the first 24-admission were correlated with a greater delirium risk ($r=0.512$, $P<0.001$) and 28-day mortality ($r=0.375$, $P<0.001$) in patients receiving 0.1–0.5 IU/kg/min insulin. Collectively, these results emerged that BGLs partially reflected the severity of the disease, with AH potentially promoting SAE and death.

Furthermore, univariate logistic analysis identified age, albumin, APACHE II score, and hyperglycemia as risk factors for delirium. Following these factors adjustments, multivariate logistic regression analysis results found hyperglycemia and age as independent risk factors for delirium. In addition, ROC analysis revealed that hyperglycemia was a predictive factor for the risk of delirium (AUC = 0.702, Fig. 1b, $P<0.001$) and 28-day mortality (AUC = 0.806, Fig. 1c, $P<0.001$).

AH exacerbates cognitive deficits, systemic inflammation, and shortened survival in septic rats

When the host immune response to infection is not well regulated, it may result in dysfunction of several organs, including SAE, which is characterized by decreased learning and memory function [2]. To estimate the BGLs implications on learning and memory function in septic rats, the *Y*-maze and NOR tests were conducted. As depicted in Fig. 2b–d, compared with the SG, the SAP of septic rats in the NG group was significantly lower (Fig. 2b, $P<0.01$), whereas their SAR was significantly greater in the *Y*-m aze (Fig. 2c, $P<0.05$), and their DI was significantly mitigated (Fig. 2d, $P<0.001$) in the NOR test, indicating severe impairment of learning and memory function in CLP rats. In addition, compared with the NG group, glucose load concentration-dependently concomitantly increased SAR and decreased SAP and DI, suggesting that AH exacerbates learning and memory impairment in septic rats. Interestingly, insulin treatment significantly improved cognitive function in the HI group, as compared with the HG group.

AH has been suggested to be linked to raised mortality rates during sepsis [28]. Next, the impact of BGLs on systemic inflammation and survival rates was investigated in septic rats. Following CLP induction for 48 h, compared

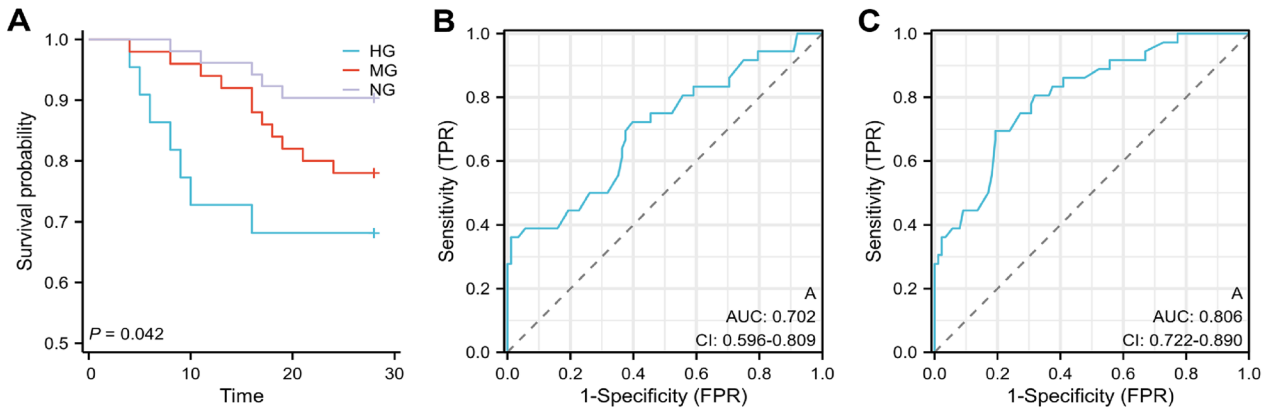

Fig. 1 **a** Kaplan–Meier survival curve for 28 days based on BGLs within the first 24 h of admission. **b**, **c** Receiver operating characteristic curve analysis of BGLs for predicting delirium and 28-day mortality

(See figure on next page.)

Fig. 2 Acute hyperglycemia (AH) exacerbates cognitive deficits, systemic inflammation, and decreased survival rates in septic rats. **a** Flowchart of the experimental protocol. Rats were chosen at random to have CLP surgery and were given intravenous infusions of a 39 mg/(kg·min) glucose solution (HG), 24 mg/(kg·min) glucose solution (MG), an equivalent amount of physiological saline (NG), or 39 mg/kg/min glucose and 0.1 IU/kg/min insulin solution (HI). They were then subjected to *Y*-m aze and NOR tests to evaluate learning and memory functions at 48 h after CLP. **b**–**d** AH further exacerbates CLP-induced learning and memory impairments. ($n=6$–8 in each group). **e**–**g** Serum levels of pro-inflammatory cytokines (IL-1β, TNF-*α*, and HMGB1) were measured using ELISA 48 h after CLP ($n=6$ in each group). **h** Changes in BGL in each group following surgery ($n=6$ in each group). **i** Survival curve and log-rank test indicate that high blood sugar significantly mitigated the mice's survival time throughout the 48 h following surgery, as opposed to the NG group. $n=15$ in each group. $^{*}P<0.05$ toward sham group, $^{¥}P<0.05$ toward NG group, $^{\$}P<0.05$ toward MG group, $^{\#}P<0.05$ toward HG group. Data are presented as mean ± SD. $^{*}P<0.05$, $^{**}P<0.01$, $^{***}P<0.001$

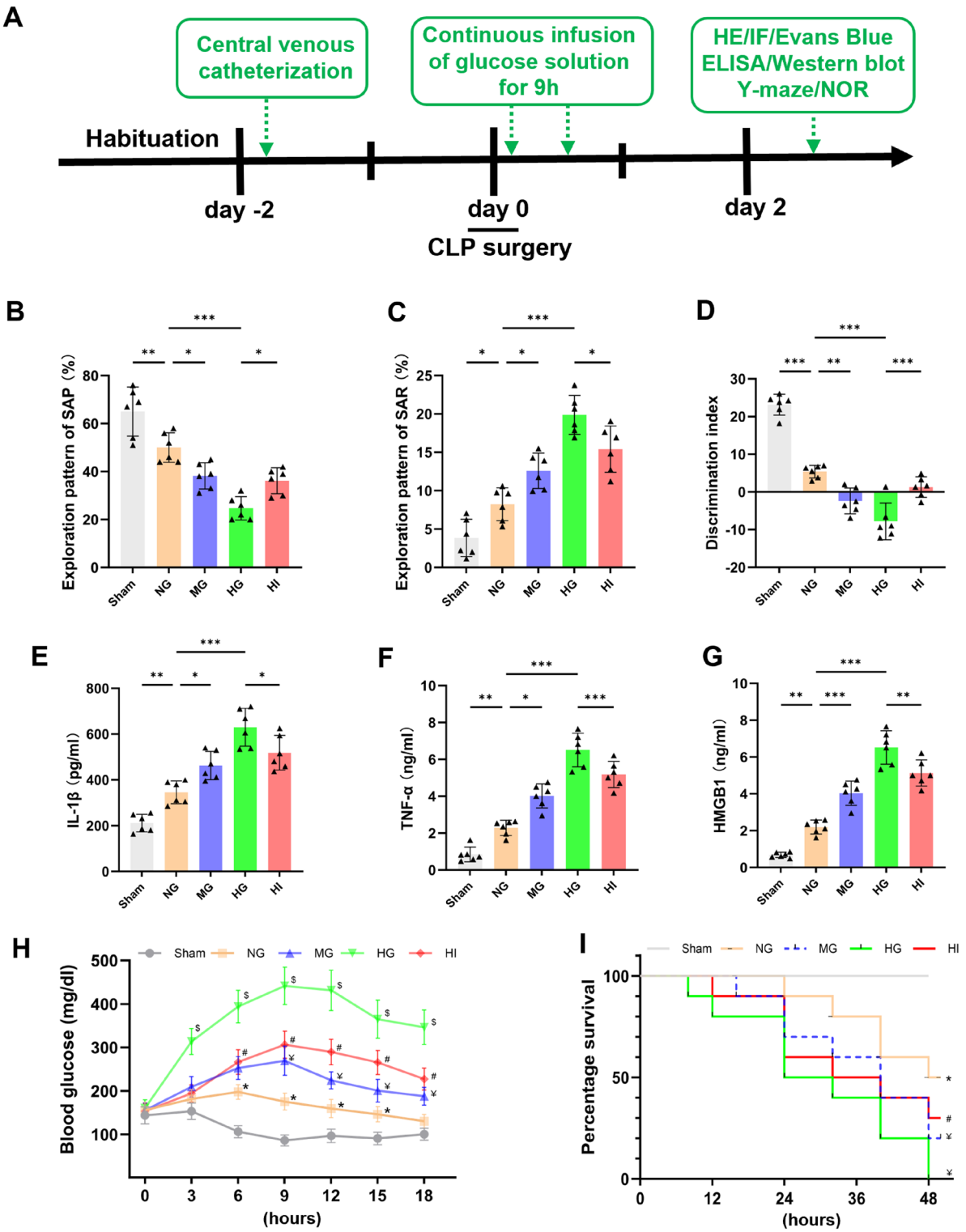

Fig. 2 (See legend on previous page.)

with the SG, the circulating inflammatory cytokines levels (IL-1β, TNF-α, and HMGB1) were significantly elevated in the NG group (Fig. 2e–g, $P<0.01$), whereas survival rates significantly declined (Fig. 2i, $P<0.05$). Glucose loads increased these inflammatory cytokines levels in a concentration-dependent manner, compared with

the NG group, leading to a reduction in survival rates. However, insulin therapy significantly ameliorated these conditions compared with the HG group. These findings collectively suggested that high BGLs exacerbate systemic inflammation and cognitive impairment in septic rats, thereby decreasing their survival rates.

AH exacerbates BBB disruption, brain tissue damage, and apoptosis in septic rats

Excessive systemic inflammation disrupts the BBB and triggers neuroinflammation, leading to cerebral damage and neuronal apoptosis [29]. To validate whether AH exacerbates these effects, brain EB content, the serum level of neuronal injury markers (NSE and S100β), and the tight junction proteins (ZO-1 and Claudin-5) expression were determined. Our findings exposed that the NG group had a significant rise in the brain EB content (Fig. 3a, $P<0.05$) and serum levels of NSE (Fig. 3b, $P<0.001$) and S100β (Fig. 3c, $P<0.01$) compared to the SG, whereas the hippocampus had a significant decline in the ZO-1 ($P<0.01$) and Claudin-5 ($P<0.05$) expression levels (Fig. 3d–f). These results conjointly indicated neuronal damage and BBB disruption in septic rats. In comparison with the NG group, both moderate and high glucose loads aggravated neuronal injury and BBB disruption. Importantly, insulin treatment reversed these effects.

Subsequently, the effects of AH on hippocampal neuropathological changes and apoptosis were examined in septic rats. As delineated in Fig. 3g, HE staining manifested that the hippocampal region of the SG exhibited a normal morphological structure with an orderly cell arrangement. In contrast, karyopycknosis, pleomorphism, and signs of neuronal vacuolation and atrophy were observed in the NG group, and the MG and HG groups had a significant rise. However, insulin treatment significantly alleviated neuronal pathological damage. In addition, TUNEL staining emerged in a greater proportion of TUNEL-positive cells in septic rats compared with the SG ($P<0.05$), which was further increased following the administration of moderate and high glucose loads (Fig. 3h–i, $P<0.001$). As anticipated, the administration of insulin resulted in a significant hindrance in the percentage of TUNEL-positive cells. Altogether, these results indicated that AH can exacerbate CLP-induced disruptions in the BBB, neuronal injury, and apoptosis.

AH enhances neuroinflammation and ChREBP expression in septic rats

Considering that excessive microglial activation is a key factor in neuroinflammation, the impact of AH on microglial activation following CLP was analyzed. Immunohistochemistry targeting IBA1 and CD68, and pro-inflammatory cytokine levels were utilized to assess microglial activation. As portrayed in Fig. 4a–e, the NG group had a significant elevation in the quantity of IBA1 + CD68-positive cells ($P<0.01$) and the levels of IL-1β ($P<0.001$), TNF-α ($P<0.01$), and HMGB1 ($P<0.01$) compared with the SG, suggesting that CLP treatment stimulated hippocampal neuroinflammation. Furthermore, moderate and high glucose exposure exacerbated neuroinflammation compared with the NG group. Nevertheless, these changes observed in the HI group were reversed by insulin treatment.

High glucose exposure reportedly upregulates ChREBP expression and increases its attaching to ChRE in the HIF-1α promoter [30]. Western blot analysis was performed to ascertain the ChREBP/HIF-1α function in AH-promoted microglial activation after CLP. Significantly, the septic rats exhibited greater expression levels of ChREBP ($P<0.05$), HIF-1α ($P<0.01$), major glycolytic enzymes HK2 and PKM2 ($P<0.05$), and the inflammatory marker iNOS ($P<0.05$), contrasted with the SG. Furthermore, these proteins expression was elevated in a concentration-dependent way by glucose loading, as compared with the NG group (Fig. 4f–k). As anticipated, these increases were significantly reduced after insulin treatment. In conclusion, these results suggested that AH may promote microglial activation following CLP by activating the ChREBP/HIF-1α pathway, thereby exacerbating neuroinflammation.

High glucose enhances the synthesis of LPS-stimulated pro-inflammatory mediators via the ChREBP/HIF-1α pathway in vitro

To further investigate the impact of high glucose on microglial activation, an in vitro experiment was conducted by treating BV2 cells with 1 μg/mL LPS and varying concentrations of glucose: 5.6 mM (LG group), 16.7 mM (MG group) or 25.0 mM (HG group). Contrasted with the con group, the group that received LPS stimulation manifested a time-dependent rise in the IL-1β, TNF-α, and HMGB1 levels while also experiencing a decrease in cell viability (Fig. 5a–c, $P<0.05$). The presence of glucose increased the generation of these inflammatory cytokines generated by LPS in a dose-dependent manner, concomitantly reducing cell viability compared with the LG group.

As glucose intake increases, microglial activation triggers metabolic reprogramming characterized by enhanced glycolysis and inhibited OXPHOS [15]. In the current study, glycolysis levels were assessed through extracellular lactate content and glucose-related metabolic pathways and by evaluating intracellular glycolytic and mitochondrial ATP levels. The results uncovered that, following LPS exposure, the LG group

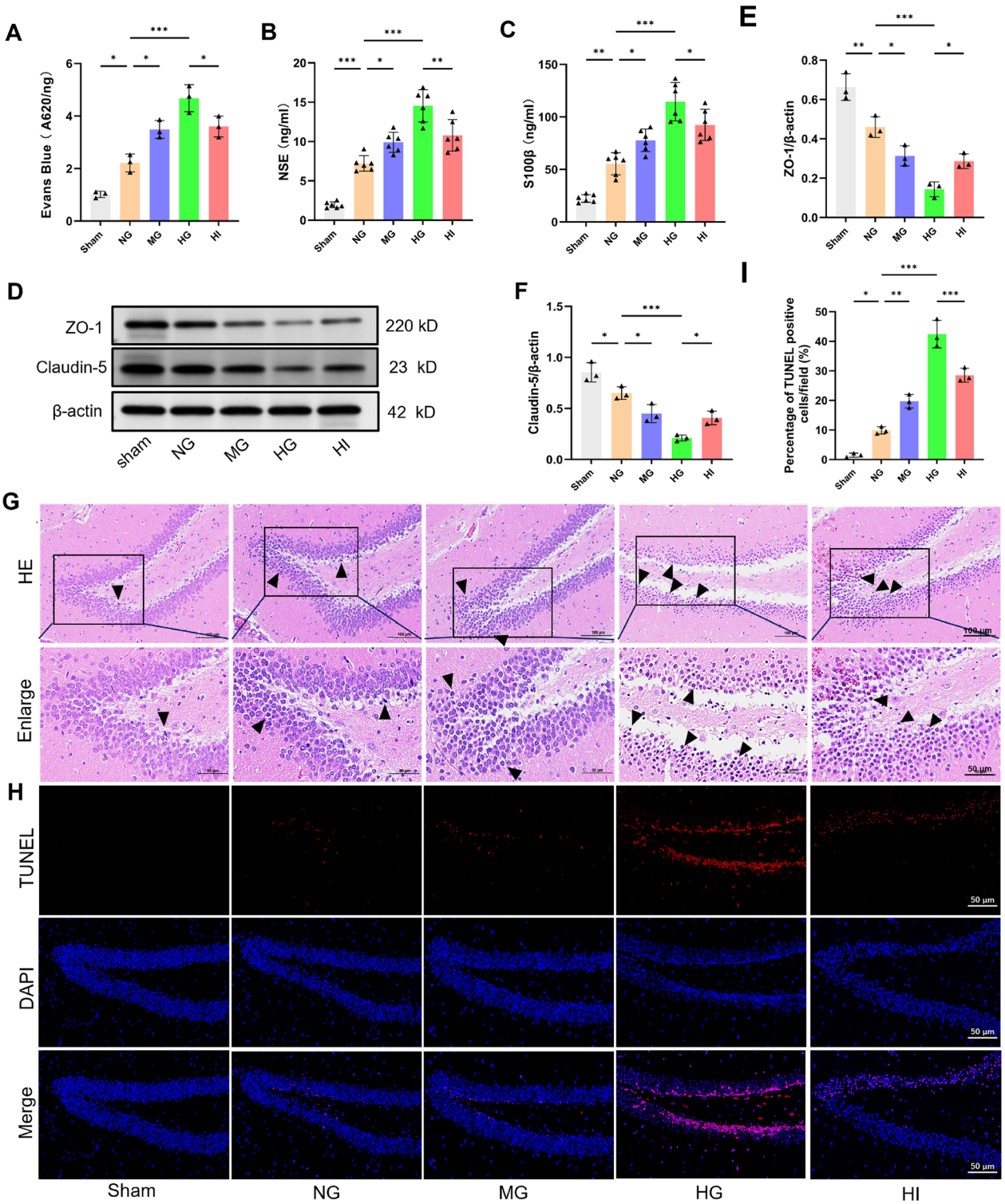

Fig. 3 AH exacerbates blood–brain barrier (BBB) disruption, brain tissue damage, and apoptosis in septic rats. **a** BBB function was assessed via the Evans Blue assay at 48 h following CLP ($n=3$ in each group). **b**, **c** Serum levels of neuronal injury markers (NSE and S100β) were quantified employing ELISA at 48 h after CLP ($n=6$ in each group). **d**–**f** Western blot assay indicated that AH decreased the ZO-1 and Claudin-5 expression levels 48 h following CLP (n = 3 in each group). **g**, **h** Hippocampal sections underwent HE and TUNEL staining 48 h after CLP. Arrowheads denote damaged neurons. **i** Quantification of TUNEL-positive cells ($n=3$ in each group). Data are presented as mean ± SD. $^{*}P<0.05$, $^{**}P<0.01$, $^{***}P<0.001$

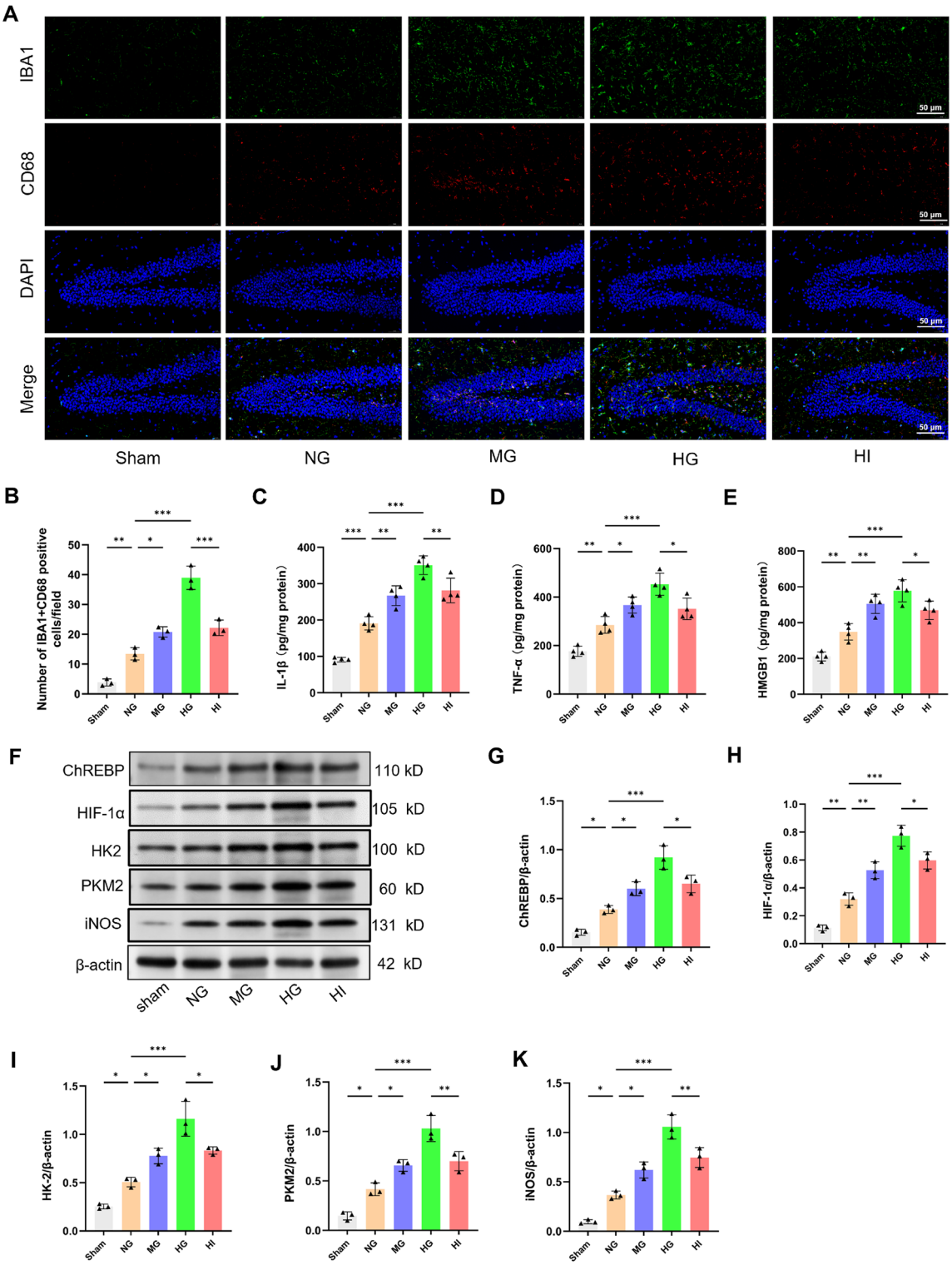

Fig. 4 AH enhances neuroinflammation and up-regulates ChREBP expression in septic rats. **a**, **b** Hippocampal sections underwent IF staining at 48 h following CLP, followed by measurement of the number of cells positive for IBA1 and CD68. **c**–**e** Hippocampal pro-inflammatory cytokines levels (IL-1β, TNF-*α*, and HMGB1) were measured 48 h after CLP. $n=4$. **f**–**k** Western blot assay indicates that AH upregulated the ChREBP, HIF-1α, HK2, PKM2, and iNOS expression 48 h after CLP. $n=3$ in each group. Data are presented as mean ± SD. $^{*}P<0.05$, $^{**}P<0.01$, $^{***}P<0.001$

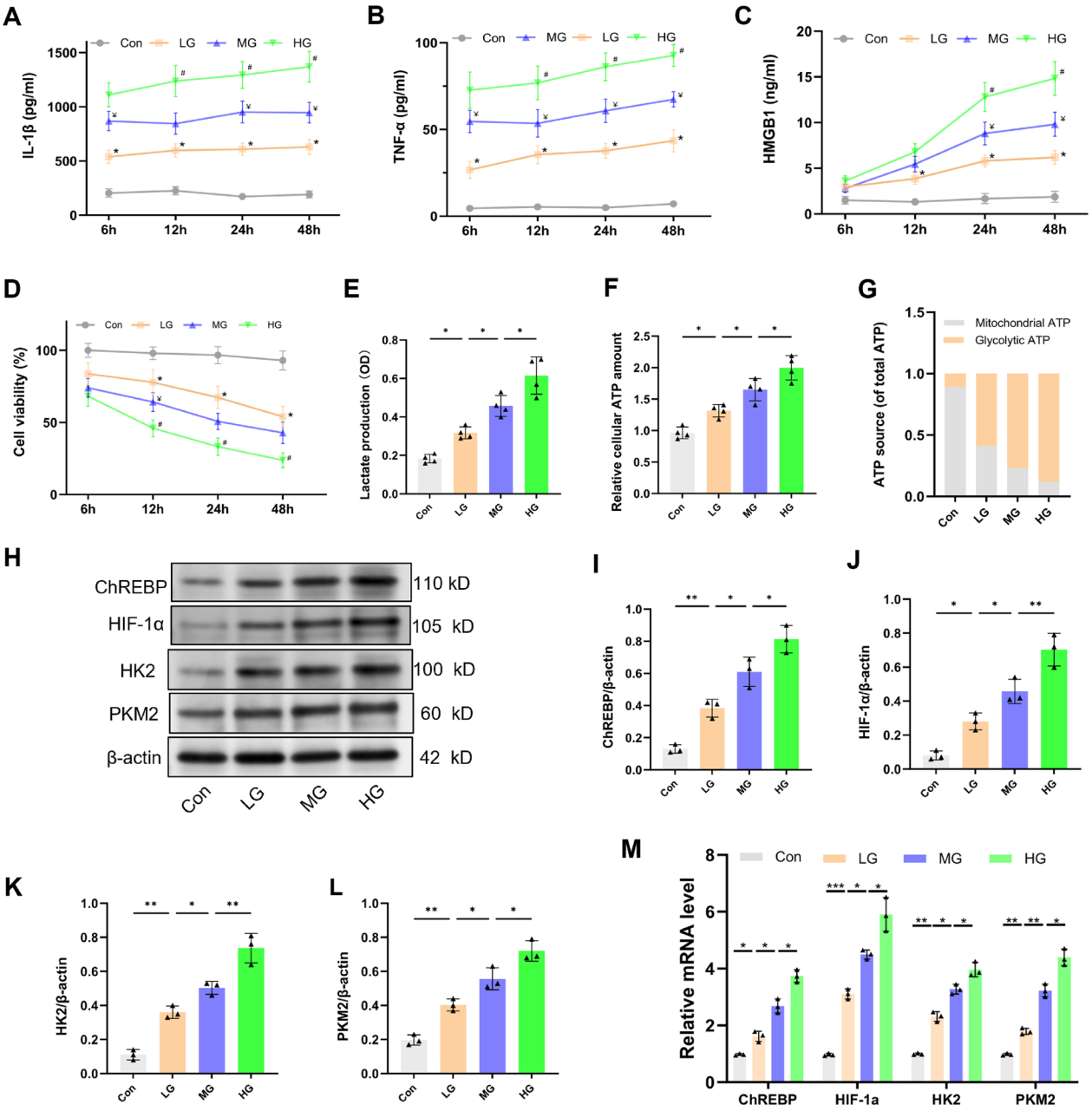

Fig. 5 High glucose enhances LPS-induced pro-inflammatory mediator production, mediated by the ChREBP/HIF-1α pathway in BV2 cells. BV2 cells underwent treatment with LPS (1 μg/mL) and 5.6 mM glucose (LG), 16.7 mM glucose (MG) or 25.0 mM glucose (HG). **a**–**d** Pro-inflammatory cytokines levels (IL-1β, TNF-*α* and HMGB1) in the supernatant and cell viability were ascertained at 6, 12, 24, and 48 h following LPS treatment. $n=4$. **e**–**g** Twelve h after treatment, extracellular lactate content, as well as intracellular glycolytic and mitochondrial ATP levels, were assessed. $n=4$. **h**–**l** Western blot assay indicates that high glucose upregulated the ChREBP, HIF-1α, HK2 and PKM2 expression 12 h after LPS treatment. **m** ChREBP, HIF-1α, HK2, and PKM2 relative mRNA levels ($n=3$ independent measurements). Data are presented as mean ± SD. $^{*}P<0.05$, $^{**}P<0.01$, $^{***}P<0.001$

had a significantly increased lactate level, relative cellular ATP levels, and the proportion of glycolytic ATP contrasted with the con group (Fig. 5e–g, $P<0.05$), indicating an increase in glycolytic flux and a shift toward LPS-induced glycolytic metabolism. Furthermore, moderate and high glucose exposure further increased glycolytic flux and metabolic shift toward glycolysis contrasted with the LG group ($P<0.05$).

Finally, the proteins and mRNA expression linked to the ChREBP/HIF-1α pathway were detected. Consistent

with the in vivo experimental results, LPS exposure upregulated the protein and mRNA expression levels of ChREBP, HIF-1α, HK2, and PKM2 as opposed to the con group (Fig. 5h–m). Compared with the LG group, moderate and high glucose treatment further upregulated these proteins and mRNA expression levels. These findings manifest that high glucose can promote microglial activation following LPS exposure by modulating the ChREBP–HIF-1α-mediated glycolytic pathway.

ChREBP knockdown prevents high glucose-evoked microglial activation following LPS exposure

To confirm the probable role of ChREBP in the microglia activation throughout sepsis caused by high hyperglycemia, BV2 cells were exposed to Lenti-ChREBP-shRNA (sh-ChREBP) or Lenti-NC (NC) treatments. We demonstrated that when comparing the NC + LPS group to the ChREBP knockdown group, there was a significant reduction in lactate levels, relative cellular ATP level, and the fraction of glycolytic ATP (Fig. 6a–c, $P < 0.01$). The sh-ChREBP + LPS + HG group emerged to significantly mitigate lactate levels, relative cellular ATP quantity, and the fraction of glycolytic ATP compared with the NC + LPS + HG group ($P < 0.001$). These findings signified that ChREBP depletion diminishes glycolytic flux and inhibits the metabolic shift toward glycolysis.

Western blot analysis revealed that the sh-ChREBP + LPS group has a significant hindrance in the HIF-1α ($P < 0.05$), HK2 ($P < 0.05$), PKM2 ($P < 0.05$), IL-1β ($P < 0.01$), TNF-α ($P < 0.01$), and HMGB1 ($P < 0.001$) protein expression level compared with the NC + LPS group (Fig. 6d–k). Furthermore, ChREBP knockdown down-regulated the expression of these proteins following LPS and high glucose stimulation compared with the NC + LPS + HG group ($P < 0.05$). In addition, in line with the western blot results, qRT-PCR analysis showed that ChREBP knockdown lowered the HIF-1α, HK2, and PKM2 mRNA levels induced by exposure to high glucose and LPS (Fig. 6l, $P < 0.001$). These outcomes emphasize the critical function of ChREBP in the inflammatory response of microglia to LPS and high glucose.

High glucose enhances the ChREBP-mediated HIF-1α pathway and promotes microglial M1 polarization in response to LPS

HIF-1α has been identified as a crucial mechanism that controls both microglial activation and metabolic reprogramming [20]. To investigate whether high glucose enhances LPS-induced microglial activation through the ChREBP-mediated HIF-1α pathway, BV2 cells pretreated with KC7F2 (10 μM), a specific inhibitor of HIF-1α, over a period of 24 h. Afterward, the cells underwent treatment with 1 μg/mL LPS and/or 25.0 mM glucose for 12 h. As illustrated in Fig. 7a–c, compared with the LPS group, high glucose exposure raised the glycolytic flux and upregulated the protein and mRNA expression levels of ChREBP, HIF-1α, HK2, PKM2, IL-1β, TNF-α, and HMGB1 (Fig. 7d–l, $P < 0.001$). Nevertheless, knocking down HIF-1α expression using KC7F2 attenuated the enhancement of glycolytic enzymes and pro-inflammatory mediators by high glucose under LPS-induced conditions ($P < 0.01$), whilst the expression of ChREBP remained unaffected. In conclusion, these results implied that high glucose further enhances sepsis-induced metabolic reprogramming and M1 polarization of microglia by activating the ChREBP/HIF-1α pathway.

Discussion

Following sepsis, infection-induced systemic inflammation can result in SAE and long-term cognitive impairment. However, research on the impact of AH on SAE is scarce. Our findings suggest that AH is linked to a greater incidence of delirium and mortality in septic patients. In addition, AH exacerbated systemic inflammation and neuroinflammation in septic rats, resulting in increased BBB permeability, cognitive deficits, and higher mortality rates. Further experiments unveiled that the underlying mechanism involves the activation of the ChREBP/HIF-1α pathway, which facilitates metabolic reprogramming and microglial activation.

The optimal blood glucose target during sepsis remains controversial despite the critical importance of effectively managing BGLs for improving outcomes [31, 32]. Previous studies have validated the detrimental effects of hyperglycemia. For example, septic patients with hyperglycemia (≥ 200 mg/dL) or stress hyperglycemia ratio (≥ 1.45) have greater mortality rates contrasted with normal BGL patients [33, 34]. In addition, AH (≥ 270 mg/dL) significantly increases circulating cytokine levels (IL-1β and TNF-α) in patients with mitigated glucose tolerance, while cytokine levels rapidly return to baseline levels in individuals with normal glucose tolerance [11, 35]. However, the mechanisms underlying these effects remain unclear. Among the 124 septic patients included in this work, those with AH (≥ 200 mg/dL) were at a significantly greater risk of developing delirium contrasted with those with well-controlled BGLs. Furthermore, septic patients with BGLs ≥ 300 mg/dL had a significantly greater mortality rate than those with normal BGLs. Further analysis identified high BGLs and age as independent risk factors for delirium, with the former capable of predicting the occurrence of delirium. These results indicate that blood glucose control may have potential benefits in mitigating the implications of hyperglycemia on the existing systemic inflammatory response.

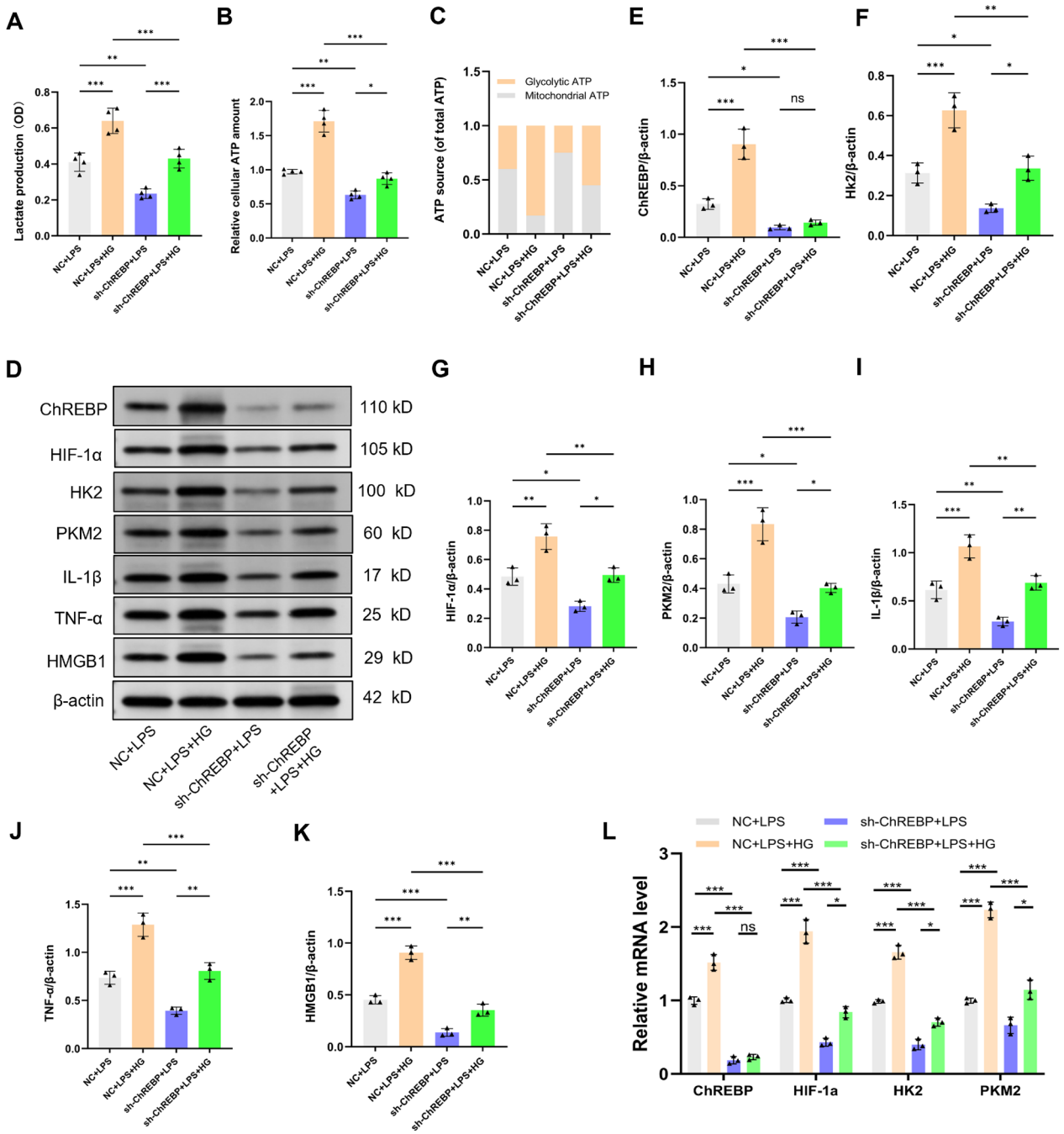

Fig. 6 ChREBP Knockdown Prevents High Glucose-evoked Microglial Activation Following Exposure to LPS. BV2 cells were exposed to lenti-ChREBP–shRNA (sh-ChREBP) or lenti-NC (NC) for 48 h, and the resulting cell lines were then subjected to screening utilizing purinomycin (5 μg/mL), subsequent treatment with LPS (1 μg/mL) and/or 25.0 mM glucose (HG). **a**–**c** 12 h after treatment, extracellular lactate content and intracellular glycolytic and mitochondrial ATP levels were assessed. $n = 4$. **d**–**k** HIF-1α, HK2, PKM2, IL-1β, TNF-*α* and HMGB1 expression level. **l** ChREBP, HIF-1α, HK2, and PKM2 relative mRNA levels (n = 3 independent measurements). Data are presented as mean ± SD. $^{*}P < 0.05$, $^{**}P < 0.01$, $^{***}P < 0.001$

Subsequently, an AH model was estimated in septic rats induced by CLP through intravenous glucose infusion. Throughout the experiment, the average BGLs in CLP rats were maintained below 180 mg/dL, in agreement with the rules of the 2021 Surviving Sepsis Campaign Guidelines [26]. Consequently, any elevations in

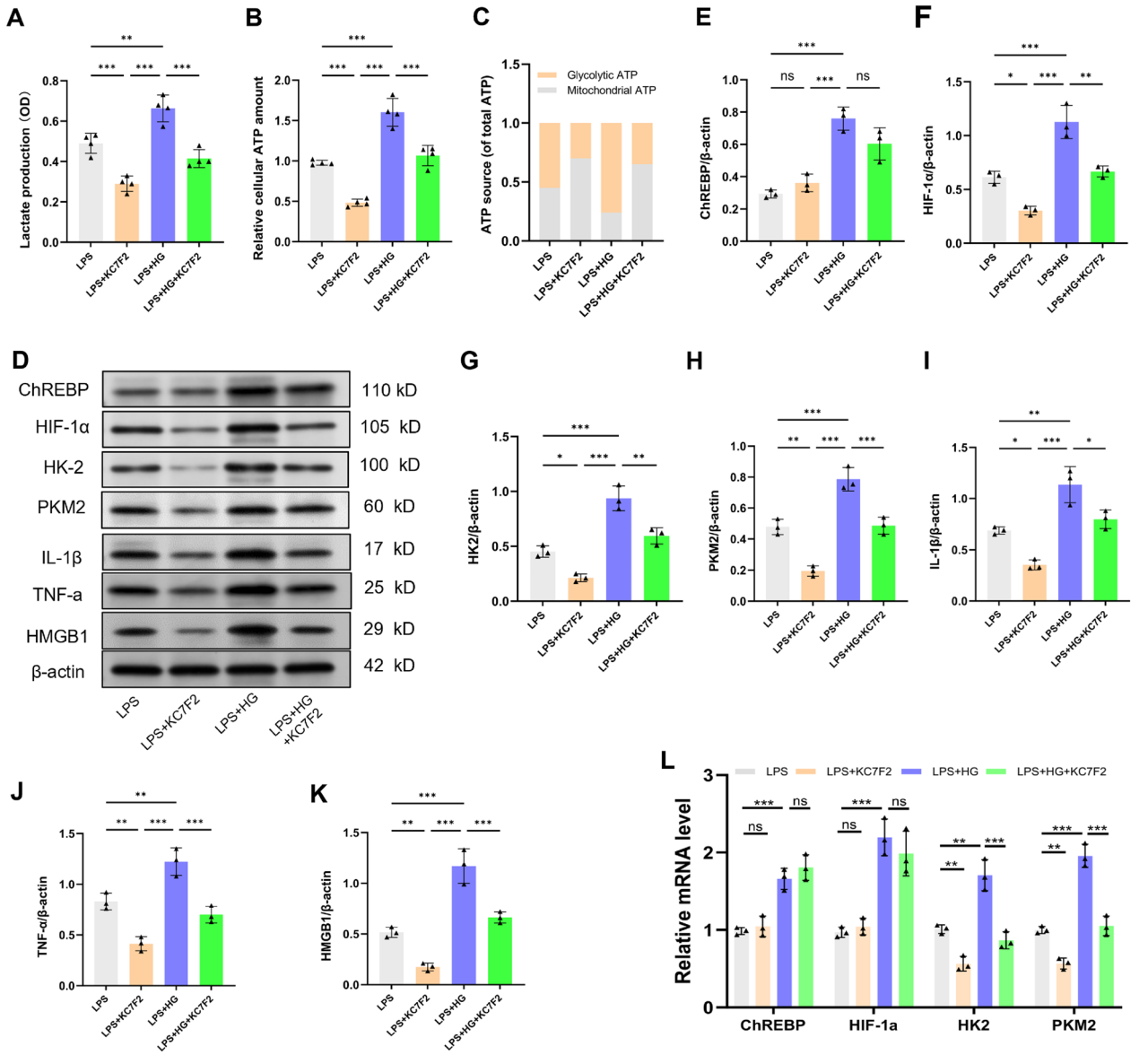

Fig. 7 Elevated glucose levels amplify the ChREBP-mediated HIF-1α pathway, leading to microglial M1 polarization responding to LPS. Prior to treatment with 1 μg/mL LPS and/or 25.0 mM glucose for 12 h, BV2 cells were pre-exposed to KC7F2 (10 μM), which is an inhibitor of HIF-1α, for 24 h. **a**–**c** Twelve hours after treatment, extracellular lactate content and intracellular glycolytic and mitochondrial ATP levels were assessed. $n = 4$. **d**–**k** HIF-1α, HK2, PKM2, IL-1β, TNF-α, and HMGB1 expression levels were measured by Western blot. **l** ChREBP, HIF-1α, HK2, and PKM2 relative mRNA levels ($n = 3$ independent measurements). Data are presented as mean ± SD. $^{*}P < 0.05$, $^{**}P < 0.01$, $^{***}P < 0.001$

the pro-inflammatory cytokines level, neuronal damage, and cognitive impairment observed in the NG group, without the influence of AH, could solely be attributed to sepsis. Our study concluded that treatment with moderate or high glucose loads increased the circulating levels of pro-inflammatory mediators by approximately 1.5 and 3 folds compared with those in septic rats, respectively. In addition, rats in the HG group exhibited more pronounced cognitive impairment and mortality compared with those in the MG and HI groups. This may be ascribed to the BGL, given that the impact of glucose sharply increases when it exceeds a particular threshold, which is estimated to be around 300 mg/dL.

Immune and metabolic disorders in SAE patients have been reported to be linked to the dysfunction of the neuroendocrine system triggered by dysregulations in the inflammatory response of the CNS, subsequently impacting key components such as the locus

coeruleus–norepinephrine system and the hypothalamic–pituitary–adrenal axis [2, 10]. Meanwhile, prolonged systemic inflammation contributes to the progression of SAE. On the one hand, circulating inflammatory mediators infiltrate the CNS through diffusion, receptor-mediated transport, or phagocytosis [36]. On the other, pro-inflammatory cytokines could disturb the neurovascular unit and tight junctions, which in turn allows neurotoxic substances and inflammatory cells to pass across the BBB [37]. We speculate that during sepsis, uncontrolled systemic inflammation, disruption of the BBB, and neuroinflammation form a vicious cycle, thereby driving neuronal damage and apoptosis. Herein, exacerbation of systemic inflammation and increased BBB permeability were noted in CLP rats after glucose loading, resulting in cognitive impairment and increased mortality rates. It is worth noting that, insulin therapy effectively reversed these conditions, suggesting that AH may disrupt the immune-inflammatory response during sepsis, with its detrimental effects attributable to exacerbations of existing inflammatory responses.

When faced with challenges such as severe infection or injury, microglia rapidly initiate a series of cellular responses, including metabolic reprogramming and phenotypic changes, to defend against threats and promote repair [14]. However, their excessive activation can lead to neuronal damage and death. Accumulating evidence has highlighted the pivotal function of HIF-1α in glycolysis and the M1 polarization of microglia [38]. According to a previous study, activation of HIF-1α has been shown to augment macrophage-mediated inflammatory cascade responses, while pharmacological inhibition of this pathway can effectively alleviate the severity of sepsis [19]. Recent studies have described that ChREBP, a key mediator activated by glucose-responsive genes, can attach to the HIF-1α promoter and participate in modulating processes such as glycolysis and immune-inflammatory responses [39]. For example, high glucose can enhance the transcriptional activity of ChREBP by binding to the glucose-responsive activation regulatory element [23] and exacerbate diabetic retinopathy by activating the ChREBP/HIF-1αpathway [39]. Conversely, ChREBP knockout effectively alleviates HIF-1α-mediated hypoxic injury [40]. Consistent with these research findings, we demonstrated that high glucose challenge upregulated the expressions of ChREBP and HIF-1α, glycolytic enzymes, and pro-inflammatory cytokines. However, this detrimental effect could be reversed by administering the HIF-1α inhibitor KC7F2 or ChREBP knockdown. These results indicate that the activation of the ChREBP/HIF-1α pathway plays a crucial role in facilitating M1 polarization and neuroinflammation in microglial cells under conditions of high glucose exposure.

This study presents several limitations. Firstly, it is a retrospective study relying on historical records, which may be prone to information bias and confounding factors, potentially constraining the ability to establish causality. Second, this study primarily examined the impact of varying blood glucose levels on neuroinflammation and delirium in septic individuals; however, additional research may be necessary in the future to determine the threshold for detrimental blood glucose levels. Finally, our findings suggest that elevated glucose levels can exacerbate the inflammatory response of microglial cells under septic conditions, potentially leading to neuronal damage and death. Nonetheless, further research is essential to elucidate the direct effects of high glucose levels on neuronal cells.

Conclusions

In summary, this research revealed that high glucose promotes neuroinflammation and delirium by enhancing microglial glycolysis and M1 polarization during sepsis, a mechanism potentially related to the upregulation of the ChREBP/HIF-1α pathway. Besides, these findings highlight the need for effective glycemic control during sepsis, considering that it may minimize the incidence of delirium and mortality in septic patients.

Supplementary Information

The online version contains supplementary material available at https://doi.org/10.1186/s40001-024-02129-3.

Additional file 1.

Acknowledgements
The authors thank the Public Platform Laboratory of the First Affiliated Hospital of Nanchang University for providing the experimental conditions and bioRender.com drawing platform.

Author contributions
Peng Yao drafted the manuscript. Ling Wu and Hao Yao collected and analyzed the data. Peng Yao and Hao Yao conduct cell experiments. Wei Shen and Ping Hu designed and supervised the study.

Funding
The study was funded by the Public Health Young-Top-notch Talent Project of Hubei Province (ShenWei), Health Commission of Hubei Province scientific research project (WJ2021M078) and Xiaogan Natural Science Program Project (XGKJ2022010025, XGKJ2024010050).

Data availability
The data presented in this study are available on reasonable request from the corresponding author.

Declarations

Ethics approval and consent to participate
All animal experimental protocols were conducted in strict adherence to the ethical guidelines established by the Animal Care and Use Committee of Nanchang University and adhered to the standards outlined by the National

Institutes of Health for the ethical care and use of laboratory animals. All methods are reported following ARRIVE guidelines for the reporting of animal experiments.

Competing interests
All authors confirm that they have no competing interests.

Author details
[1]Affiliated Rehabilitation Hospital, Jiang Xi Medical College, Nanchang University, Nanchang 330003, Jiangxi, China. [2]Department of Critical Care Medicine, Xiaogan Hospital Affiliated to Wuhan University of Science and Technology, Xiaogan 432000, Hubei, China. [3]The First Affiliated Hospital of Nanchang University, Jiang Xi Medical College, Nanchang University, Nanchang 330003, Jiangxi, China.

Received: 12 September 2024 Accepted: 25 October 2024
Published online: 14 November 2024

References

1. Zhou Y, Bai L, Tang W, Yang W, Sun L. Research progress in the pathogenesis of sepsis-associated encephalopathy. Heliyon. 2024;10:e33458. https://doi.org/10.1016/j.heliyon.2024.e33458.
2. Hong Y, Chen P, Gao J, Lin Y, Chen L, Shang X. Sepsis-associated encephalopathy: from pathophysiology to clinical management. Int Immunopharmacol. 2023;124:110800. https://doi.org/10.1016/j.intimp.2023.110800.
3. Zhang Z, Guo L, Jia L, Duo H, Shen L, Zhao H. Factors contributing to sepsis-associated encephalopathy: a comprehensive systematic review and meta-analysis. Front Med (Lausanne). 2024;11:1379019. https://doi.org/10.3389/fmed.2024.1379019.
4. Chung HY, Wickel J, Hahn N, Mein N, Schwarzbrunn M, Koch P, Ceanga M, Haselmann H, Baade-Büttner C, von Stackelberg N, et al. Microglia mediate neurocognitive deficits by eliminating C1q-tagged synapses in sepsis-associated encephalopathy. Sci Adv. 2023;9:eabq7806. https://doi.org/10.1126/sciadv.abq7806.
5. Yin XY, Tang XH, Wang SX, Zhao YC, Jia M, Yang JJ, Ji MH, Shen JC. HMGB1 mediates synaptic loss and cognitive impairment in an animal model of sepsis-associated encephalopathy. J Neuroinflammation. 2023;20:69. https://doi.org/10.1186/s12974-023-02756-3.
6. Carrasco-Sánchez FJ, Carretero-Gómez J, Gómez-Huelgas R, Garcia-Ordoñez MA, Pardo-Ortega MV, de Escalante-Yanguela B, Mateos-Polo L, Formiga F, Ena J. Stress-induced hyperglycemia on complications in non-critically elderly hospitalized patients. Rev Clin Esp (Barc). 2018;218:223–31. https://doi.org/10.1016/j.rce.2018.02.017.
7. Fujishima S, Gando S, Saitoh D, Kushimoto S, Ogura H, Abe T, Shiraishi A, Mayumi T, Sasaki J, Kotani J, et al. Incidence and impact of dysglycemia in patients with sepsis under moderate glycemic control. Shock. 2021;56:507–13. https://doi.org/10.1097/shk.0000000000001794.
8. Zhang S, Zhang Y, Wen Z, Yang Y, Bu T, Bu X, Ni Q. Cognitive dysfunction in diabetes: abnormal glucose metabolic regulation in the brain. Front Endocrinol (Lausanne). 2023;14:1192602. https://doi.org/10.3389/fendo.2023.1192602.
9. Biessels GJ, Despa F. Cognitive decline and dementia in diabetes mellitus: mechanisms and clinical implications. Nat Rev Endocrinol. 2018;14:591–604. https://doi.org/10.1038/s41574-018-0048-7.
10. Bar-Or D, Rael LT, Madayag RM, Banton KL, Tanner A, Acuna DL, Lieser MJ, Marshall GT, Mains CW, Brody E. Stress hyperglycemia in critically Ill patients: insight into possible molecular pathways. Front Med (Lausanne). 2019;6:54. https://doi.org/10.3389/fmed.2019.00054.
11. Yu WK, Li WQ, Li N, Li JS. Influence of acute hyperglycemia in human sepsis on inflammatory cytokine and counterregulatory hormone concentrations. World J Gastroenterol. 2003;9:1824–7. https://doi.org/10.3748/wjg.v9.i8.1824.
12. Ingels C, Derese I, Wouters PJ, Van den Berghe G, Vanhorebeek I. Soluble RAGE and the RAGE ligands HMGB1 and S100A12 in critical illness: impact of glycemic control with insulin and relation with clinical outcome. Shock. 2015;43:109–16. https://doi.org/10.1097/shk.0000000000000278.
13. Guo Q, Gobbo D, Zhao N, Zhang H, Awuku NO, Liu Q, Fang LP, Gampfer TM, Meyer MR, Zhao R, et al. Adenosine triggers early astrocyte reactivity that provokes microglial responses and drives the pathogenesis of sepsis-associated encephalopathy in mice. Nat Commun. 2024;15:6340. https://doi.org/10.1038/s41467-024-50466-y.
14. Hu Y, Mai W, Chen L, Cao K, Zhang B, Zhang Z, Liu Y, Lou H, Duan S, Gao Z. mTOR-mediated metabolic reprogramming shapes distinct microglia functions in response to lipopolysaccharide and ATP. Glia. 2020;68:1031–45. https://doi.org/10.1002/glia.23760.
15. Orihuela R, McPherson CA, Harry GJ. Microglial M1/M2 polarization and metabolic states. Br J Pharmacol. 2016;173:649–65. https://doi.org/10.1111/bph.13139.
16. Yang Y, Ke J, Cao Y, Gao Y, Lin C. Melatonin regulates microglial M1/M2 polarization via AMPKα2-mediated mitophagy in attenuating sepsis-associated encephalopathy. Biomed Pharmacother. 2024;177:117092. https://doi.org/10.1016/j.biopha.2024.117092.
17. Yu H, Kan J, Tang M, Zhu Y, Hu B. Lipopolysaccharide preconditioning restricts microglial overactivation and alleviates inflammation-induced depressive-like behavior in mice. Brain Sci. 2023. https://doi.org/10.3390/brainsci13040549.
18. Bejoy J, Yuan X, Song L, Hua T, Jeske R, Sart S, Sang QA, Li Y. Genomics analysis of metabolic pathways of human stem cell-derived microglia-like cells and the integrated cortical spheroids. Stem Cells Int. 2019;2019:2382534. https://doi.org/10.1155/2019/2382534.
19. Guan S, Sun L, Wang X, Huang X, Luo T. Propofol inhibits neuroinflammation and metabolic reprogramming in microglia in vitro and in vivo. Front Pharmacol. 2023;14:1161810. https://doi.org/10.3389/fphar.2023.1161810.
20. Yang L, Xie M, Yang M, Yu Y, Zhu S, Hou W, Kang R, Lotze MT, Billiar TR, Wang H, et al. PKM2 regulates the Warburg effect and promotes HMGB1 release in sepsis. Nat Commun. 2014;5:4436. https://doi.org/10.1038/ncomms5436.
21. Peyssonnaux C, Cejudo-Martin P, Doedens A, Zinkernagel AS, Johnson RS, Nizet V. Cutting edge: essential role of hypoxia inducible factor-1alpha in development of lipopolysaccharide-induced sepsis. J Immunol. 2007;178:7516–9. https://doi.org/10.4049/jimmunol.178.12.7516.
22. Zhang C, Steadman M, Santos HP Jr, Shaikh SR, Xavier RM. GPAT1 activity and abundant palmitic acid impair insulin suppression of hepatic glucose production in primary mouse hepatocytes. J Nutr. 2024;154:1109–18. https://doi.org/10.1016/j.tjnut.2024.02.004.
23. Isoe T, Makino Y, Mizumoto K, Sakagami H, Fujita Y, Honjo J, Takiyama Y, Itoh H, Haneda M. High glucose activates HIF-1-mediated signal transduction in glomerular mesangial cells through a carbohydrate response element binding protein. Kidney Int. 2010;78:48–59. https://doi.org/10.1038/ki.2010.99.
24. Guo S, Bragina O, Xu Y, Cao Z, Chen H, Zhou B, Morgan M, Lin Y, Jiang BH, Liu KJ, et al. Glucose up-regulates HIF-1 alpha expression in primary cortical neurons in response to hypoxia through maintaining cellular redox status. J Neurochem. 2008;105:1849–60. https://doi.org/10.1111/j.1471-4159.2008.05287.x.
25. Guo B, Qi M, Luo X, Guo L, Xu M, Zhang Y, Li Z, Li M, Wu R, Guan T, et al. GIP attenuates neuronal oxidative stress by regulating glucose uptake in spinal cord injury of rat. CNS Neurosci Ther. 2024;30:e14806. https://doi.org/10.1111/cns.14806.
26. Evans L, Rhodes A, Alhazzani W, Antonelli M, Coopersmith CM, French C, Machado FR, McIntyre L, Ostermann M, Prescott HC, et al. Surviving sepsis campaign: international guidelines for management of sepsis and septic shock 2021. Intensive Care Med. 2021;47:1181–247. https://doi.org/10.1007/s00134-021-06506-y.
27. Yamazaki H, Onoyama S, Gotani S, Deguchi T, Tamura M, Ohta H, Iwano H, Nishida H, Dickinson PJ, Akiyoshi H. Influence of the hypoxia-activated prodrug evofosfamide (TH-302) on glycolytic metabolism of canine glioma: a potential improvement in cancer metabolism. Cancers (Basel). 2023. https://doi.org/10.3390/cancers15235537.
28. Oh AR, Lee DY, Lee S, Lee JH, Yang K, Choi B, Park J. Association between preoperative glucose dysregulation and delirium after non-cardiac surgery. J Clin Med. 2024. https://doi.org/10.3390/jcm13040932.
29. Gao Q, Hernandes MS. Sepsis-associated encephalopathy and blood-brain barrier dysfunction. Inflammation. 2021;44:2143–50. https://doi.org/10.1007/s10753-021-01501-3.
30. Chang ML, Chiu CJ, Shang F, Taylor A. High glucose activates ChREBP-mediated HIF-1α and VEGF expression in human RPE cells under

normoxia. Adv Exp Med Biol. 2014;801:609–21. https://doi.org/10.1007/978-1-4614-3209-8_77.
31. Cai W, Xu J, Wu X, Chen Z, Zeng L, Song X, Zeng Y, Yu F. Association between triglyceride-glucose index and all-cause mortality in critically ill patients with ischemic stroke: analysis of the MIMIC-IV database. Cardiovasc Diabetol. 2023;22:138. https://doi.org/10.1186/s12933-023-01864-x.
32. Poole AP, Finnis ME, Anstey J, Bellomo R, Bihari S, Biradar V, Doherty S, Eastwood G, Finfer S, French CJ, et al. The effect of a liberal approach to glucose control in critically Ill patients with type 2 diabetes: a multicenter, parallel-group, open-label randomized clinical trial. Am J Respir Crit Care Med. 2022;206:874–82. https://doi.org/10.1164/rccm.202202-0329OC.
33. Lu Z, Tao G, Sun X, Zhang Y, Jiang M, Liu Y, Ling M, Zhang J, Xiao W, Hua T, et al. Association of blood glucose level and glycemic variability with mortality in sepsis patients during ICU hospitalization. Front Public Health. 2022;10:857368. https://doi.org/10.3389/fpubh.2022.857368.
34. Yan F, Chen X, Quan X, Wang L, Wei X, Zhu J. Association between the stress hyperglycemia ratio and 28-day all-cause mortality in critically ill patients with sepsis: a retrospective cohort study and predictive model establishment based on machine learning. Cardiovasc Diabetol. 2024;23:163. https://doi.org/10.1186/s12933-024-02265-4.
35. Esposito K, Nappo F, Marfella R, Giugliano G, Giugliano F, Ciotola M, Quagliaro L, Ceriello A, Giugliano D. Inflammatory cytokine concentrations are acutely increased by hyperglycemia in humans: role of oxidative stress. Circulation. 2002;106:2067–72. https://doi.org/10.1161/01.cir.0000034509.14906.ae.
36. Althubaity N, Schubert J, Martins D, Yousaf T, Nettis MA, Mondelli V, Pariante C, Harrison NA, Bullmore ET, Dima D, et al. Choroid plexus enlargement is associated with neuroinflammation and reduction of blood brain barrier permeability in depression. Neuroimage Clin. 2022;33:102926. https://doi.org/10.1016/j.nicl.2021.102926.
37. Pan S, Lv Z, Wang R, Shu H, Yuan S, Yu Y, Shang Y. Sepsis-induced brain dysfunction: pathogenesis, diagnosis, and treatment. Oxid Med Cell Longev. 2022;2022:1328729. https://doi.org/10.1155/2022/1328729.
38. de Souza Stork S, Hübner M, Biehl E, Danielski LG, Bonfante S, Joaquim L, Denicol T, Cidreira T, Pacheco A, Bagio E, et al. Diabetes exacerbates sepsis-induced neuroinflammation and brain mitochondrial dysfunction. Inflammation. 2022;45:2352–67. https://doi.org/10.1007/s10753-022-01697-y.
39. Owczarek A, Gieczewska KB, Jarzyna R, Frydzinska Z, Winiarska K. Transcription factor ChREBP mediates high glucose-evoked increase in HIF-1α content in epithelial cells of renal proximal tubules. Int J Mol Sci. 2021. https://doi.org/10.3390/ijms222413299.
40. Li L, Long J, Mise K, Poungavrin N, Lorenzi PL, Mahmud I, Tan L, Saha PK, Kanwar YS, Chang BH, et al. The transcription factor ChREBP links mitochondrial lipidomes to mitochondrial morphology and progression of diabetic kidney disease. J Biol Chem. 2023;299:105185. https://doi.org/10.1016/j.jbc.2023.105185.

Publisher's Note